Short-term velocity and water-pressure variations down-glacier from a riegel, Storglaciären, Sweden

Brian Hanson,[1] Roger LeB. Hooke,[2] Edmund M. Grace, Jr[1]
[1]Department of Geography, University of Delaware, Newark, Delaware 19716, U.S.A.
[2]Department of Geology and Geophysics, University of Minnesota, Minneapolis, Minnesota 55455, U.S.A.

ABSTRACT. During the 1991–94 summer field seasons, time-correlated measurements of water pressure and surface speed were made over and down-glacier from a major riegel on Storglaciären, Sweden. Measurements were made at sub-hourly time-scales in order to discern details in the diurnal cycle. Large water-input events, typically associated with rain storms, produced coherent, lagged surface-velocity responses that could be understood in terms of till deformation or decoupling, and these have been discussed elsewhere. The consequences of smaller diurnal water-pressure events were more enigmatic, in that acceleration of ice flow generally preceded the onset of the local water-pressure rise. From consideration of these data and other work done on the hydrology of Storglaciären, we infer that the ice in this area is generally pushed from behind via a relaxation in extensional strain across the riegel. Hence, accelerations occur in response to increases in water pressure that occur up-glacier and that precede local water-pressure rises. In addition, following a period of large storm events, surface speeds became more spatially coherent and were in phase with the diurnal water-pressure cycle. This suggests that the large water-pressure events lead to a spatially more homogeneous subglacial drainage system. Sliding laws need to take into account such temporal changes in spatial coherence of the subglacial drainage system.

INTRODUCTION

Subglacial water pressures are presumed to affect the basal velocity of the ice. The sliding law commonly takes the form

$$u_b = \frac{f(\tau_b)}{g(p_i, p_w)} \quad (1)$$

with variations depending on the formulator's opinion of the governing physical processes. Here, u_b is basal sliding rate, τ_b is basal drag, p_i and p_w are ice and water pressures, respectively, and f and g are functions: f usually monotonically increasing with τ_b and g usually monotonically decreasing with $p_i - p_w$. The generic form of Equation (1) seems to be common to formulations based on sliding of ice over bare rock (Weertman, 1957) or over a non-deforming till layer (Hooke and others, 1997). Some of the earliest field data supporting the hypothesis that velocities are influenced by subglacial water pressure were obtained by Hodge (1974) working on Nisqually Glacier. Subsequently, combined measurements of speed and water pressure on Findelengletscher (Iken and Bindschadler, 1986; Iken and Truffer, 1997), Variegated Glacier (Kamb and Engelhardt, 1987) and Storglaciären (Jansson and Hooke, 1989; Jansson, 1995) have demonstrated that speed responds to water-pressure variations that last at least a few days. When sliding speed on Trapridge Glacier was measured directly along with internal water pressure on sub-diurnal time-scales, peaks in speed and water pressure were not in phase (Blake and others, 1994). On Storglaciären, field measurements that resolve water pressure and surface velocity on sub-hourly time-scales show a diverse array of responses and non-responses. The purpose of this paper is to present some of these Storglaciären data and to discuss some possible processes by which the simple idea of Equation (1) may be obscured when dealing with short time-scales.

STORGLACIÄREN BACKGROUND

Storglaciären (Fig. 1) is a small valley glacier in northern Sweden for which there is a photographic record extending back to ~1880. Modern scientific studies on it began in 1946 when Schytt (1959, 1981) initiated still-continuing mass-balance measurements. Recent papers have discussed its bed topography (Eriksson and others, 1993) and composition (Brand and others, 1987), mass balance (Holmlund, 1987, 1988), temperature regime (Hooke and others, 1983a, Holmlund and Eriksson, 1989), internal deformation (Hooke and others, 1992), hydrology (Hooke and others, 1988; Seaberg and others, 1988; Hock and Hooke, 1993; Kohler, 1995), surface deformation and flow (Hooke and others 1983b, 1989; Jansson and Hooke, 1989; Hanson and Hooke, 1994) and basal till deformation (Hooke and others, 1997; Iverson and others, 1995). Some of the data discussed here were used in these last two papers. For a review of recent work on Storglaciären's dynamics and hydrology, see Jansson (1996).

Most of Storglaciären is composed of temperate ice but it has a perennially cold ($<0°C$) surface layer, up to 60 m thick, in its ablation zone (Holmlund and Eriksson, 1989). Ice in this cold layer is impermeable. Water thus reaches the englacial part of the drainage system principally by way of crevasses and moulins that extend through the cold layer. The two primary areas for such water input are the

https://doi.org/10.3189/S0022143000002689 Published online by Cambridge University Press

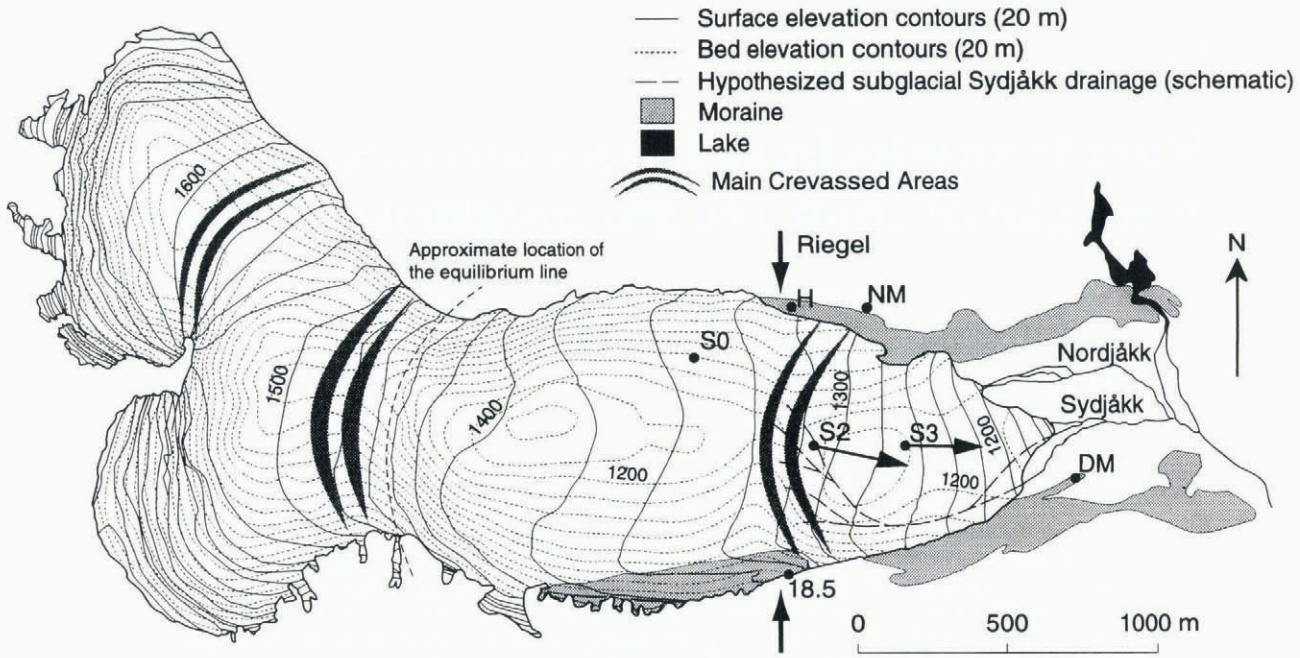

Fig. 1. Map of Storglaciären showing surface and bed topography (contours in m a.s.l.); locations of stakes (S0, S1, S2 and S3), fixed points (NM and 18.5), and distance-meter sites (DM and H) discussed in text; and inferred subglacial drainage in Sydjåkk. Velocity vectors on S2 and S3 show direction and relative size of surveyed 1992 summer speeds; see Table 2 for actual vector values.

crevasse field near the equilibrium line and moulins in the crevasse zone over the riegel (transverse bedrock ridge) near the middle of the ablation area (Fig. 1). Tracer (Seaberg and others, 1988) and detailed water-balance studies (Cutler, 1997) indicate that the two outlet streams, Nordjåkk and Sydjåkk, have differing sources. Surface streams that enter the glacier in the mid-ablation-area crevasse zone flow out via Sydjåkk, while surface water produced in the accumulation area and feeding englacial and subglacial conduits in the upper part of the ablation area drains largely via Nordjåkk, although Cutler (1997) found evidence that some of this water drains to Sydjåkk early in the melt season. Storglaciären thus has a complicated internal drainage system, varying both spatially and temporally.

Hooke and others (1989) presented the results of a multi-year surface-velocity monitoring project covering the entire glacier and these results were used by Hanson (1995) to infer the stress field. From these studies, we have established a few basic background facts. The main flow on Storglaciären arises from accumulation in the north cirque, achieves highest speeds (~100 mm d^{-1} annual average) in a steep zone at the base of the accumulation zone, swings left at and below the equilibrium line, mostly has speeds of 40–50 mm d^{-1} (annual average) near the center line in the main overdeepening, and then becomes compressive a short distance down-glacier from the riegel as ice slows near the toe. In the area discussed here (S2 and S3, Fig. 1), summer speeds are about 40 mm d^{-1} on average but S2 is in an area of extending flow just below a crevassed zone, whereas S3 is in an area of compressive flow.

From borehole inclinometry and interseasonal velocity changes (Hooke and others, 1989, 1992), we infer that internal deformation accounts for a small fraction of the total surface speed, perhaps 10 mm d^{-1} and certainly less than 20 mm d^{-1}. Velocity changes shown in our data are thus ascribed entirely to changes in sliding speed.

FIELD MEASUREMENTS

Velocity measurements

The primary data analyzed here are water pressures and surface speeds (Fig. 2). The measurements were made during field seasons lasting from late June to late July in 1991 and 1992, and from early July to mid-August 1993 and 1994 (Table 1). Distance data were collected using Automatic Distance Measurement (ADM) systems, each consisting of an infrared laser range finder controlled by a pocket-sized computer that also serves as a data logger (described in Hanson and Hooke (1994)). In 1991, one such system was placed on a stationary rock near the south side of the glacier (DM, Fig. 1) and aimed at a triple prism at site 2 (S2). Two ADMs were deployed from 1992 onward. In 1992 and 1993, velocity (V) measurements were made from DM to S3 (V 92–S3, V 93–S3) and strain-rate (SR) data were obtained between S2 and S3, using a distance meter anchored to stakes at S2 (SR 92, SR 93; Table 1). In 1994, speeds at S2 were again measured from DM and speeds at a new site, S0, were also measured from a distance meter located on the north moraine (H, Fig. 1).

Points on the glacier consisted of 5 cm diameter iron pipes, 6 m long, that were drilled 4–5 m into the ice. All of these had more than 3 m still embedded in the ice at the end of the season, so they all remained firmly anchored, although increasingly capable of swaying, throughout the period of measurements. The distance meter at S2 was fixed to three such stakes, drilled in a firmly cross-braced triangle approximately 70 cm on a side.

Distance measurements were attempted every 10 min, with more frequent attempts made if visibility prevented a scheduled measurement. Gaps in the measurement series are caused by technical problems, primarily battery failures, and weather-related visibility problems. Visibility fail-

https://doi.org/10.3189/S0022143000002689 Published online by Cambridge University Press

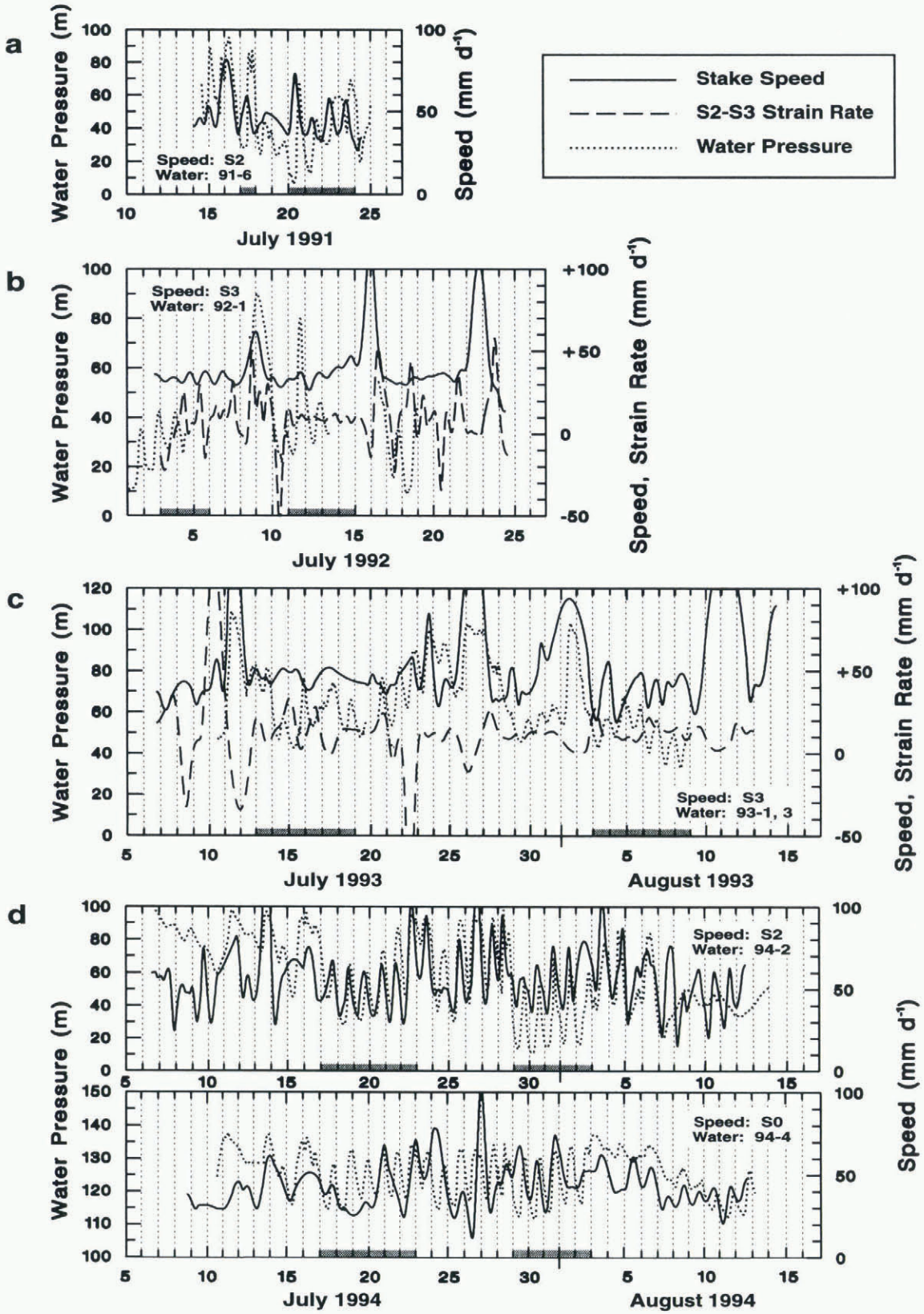

Fig. 2. ADM speeds, ADM strain rates and water-pressure measurements. Vertical scale on speed/strain-rate axes is the same for all diagrams; water-pressure scale varies. Water pressures are given as height above the bed of the water level in the borehole. Some data series are truncated (in time) from the periods listed in Table 1 in order to highlight the periods of correlated measurements. In (b) and (c), strain rate is shown as the rate at which S2 and S3 were getting closer; positive is compressive. (a) 1991: all measurements at S2. (b) 1992: speed at S3, water at S2, S2–S3 strain rate included. (c) 1993: speed at S3, water at S2 until 20 July and at S2.5 thereafter, S2–S3 strain rate included. (d) 1994: upper diagram is S2 speed and water, lower diagram is S0 speed and water. Shaded bars on the time axis indicate periods averaged to form the diurnal composite diagrams (Fig. 3).

ures caused by fog or precipitation were common when shooting the >800 m distance from DM to S2. Visibility from DM to S3 or H to S0 was only interrupted in the most severe rain storms, which did, nevertheless, result in very interesting water-pressure events. Strain-rate measurements from S2 to S3 were never interrupted for significant lengths of time by weather, owing to the short distance of measurement.

https://doi.org/10.3189/S0022143000002689 Published online by Cambridge University Press

Table 1. Data series collected for short-term velocity and borehole water pressure

Automated distance measurements				
Name	*Date begun*	*Date ends*	*Distance*	*Measurement line*
			m	
V 91–S2	6 Jul 1991	24 Jul 1991	835	DM to S2
V 92–S3	2 Jul 1992	24 Jul 1992	562	DM to S3
SR 92	2 Jul 1992	24 Jul 1992	274	S2 to S3
V 93–S3	6 Jul 1993	14 Aug 1993	550	DM to S3
SR 93	6 Jul 1993	13 Aug 1993	271	S2 to S3
V 94–S2	6 Jul 1994	12 Aug 1994	814	DM to S2
V 94–S0	8 Jul 1994	12 Aug 1994	410	H to S0

Borehole water pressures				
Name	*Date begun*	*Date ends*	*Hole depth*	*Location*
			m	
WP 91–6	14 Jul 1991	25 Jul 1991	119.6	S2
WP 92–1	28 June 92	18 Jul 1992	121.4	S2
WP 92–3	3 Jul 1992	11 Jul 1992	96.6	S3
WP 93–1	10 Jul 1993	21 Jul 1993	122.7	S2
WP 93–3	20 Jul 1993	8 Aug 1993	118.3	S2.5*
WP 93–5	14 Jul 1993	22 Jul 1993	91.6	S3
WP 94–2	6 Jul 1994	26 Sep 1994	115.2	S2
WP 94–4	10 Jul 1994	26 Sep 1994	151.2	S0

* S2.5 is roughly half-way between S2 and S3. It was used for water pressure only in 1993.

The ADM data were supplemented by three-dimensional surveys from the base lines NM–18.5 or H–18.5 (Fig. 1), using an electronic theodolite and distance meter. These surveys were made nine–ten times in each field season (every 2–3 days as weather permitted) (Table 2). They provided directions of motion for each of the stakes and were made sufficiently often to show that the direction does not vary appreciably during acceleration events. Thus, the events shown by the ADM experiments appear to consist of speed changes only, without accompanying directional change, at least within the limits of these surveys.

Table 2. Summary of three-dimensional surveys of stakes used for ADM experiments. (a) Speeds in mm d^{-1}, horizontal azimuth relative to due east, vertical direction relative to the horizontal plane

Stake	*Year*	*Horizontal speed*	*Vertical speed*	*Total speed*	*Horizontal azimuth*	*Vertical direction*
S2	1991	50.0	−8.7	50.7	−11.5°	−9.8°
S2	1992	48.7	−6.2	49.1	−9.9°	−7.3°
S2	1993	66.3	−13.0	67.5	−12.1°	−13.7°
S3	1991	42.6	+1.1	42.6	+0.3°	+1.5°
S3	1992	39.8	+1.0	39.8	−1.4°	+1.5°
S3	1993	58.4	+3.7	58.6	+0.7°	+4.5°
S2	1994	57.7	−2.1	57.7	−10.7°	−2.3°
S0	1994	47.6	7.1	48.1	−1.0°	+9.4°

(b) Directions of motion relative to lines measured by ADM. 1992 measurements for S2 and S3, 1994 for S0

	Horizontal	*Vertical*
S2 towards DM	1.4° to right	1.9° upward
S3 towards DM	9.8° to left	10.9° upward
S2 towards S3	6.8° to right	1.3° downward
S0 towards H	38.7° to right	4.1° upward

Speeds calculated as first derivatives of ADM distance data are based on the directly measured distance changes; they were not "corrected" for angles between the measurement line and the direction of motion of the stake. For S2 and S3, the stakes primarily discussed in this paper, the angles between the actual motion of surveyed stakes and the components of that motion directly towards the distance meter are very small anyway (Table 2b).

Corrections for temporal changes in atmospheric density were applied to the distance measurements. The temperatures required for this calculation were measured beneath a data-logger shelter directly at S2 during much of the 1991 season. During the remainder of the 1991 season and the entire 1992 season, temperatures were taken from a weather station higher on the glacier. Temperatures for 1993 and 1994 were obtained from a station maintained ~200 m down-glacier from S3. All of these temperature stations were within the same sun and shade conditions as the sight line of the distance meter for nearly all of the day. Cutler (1997) showed that meteorological stations within the larger region of the main overdeepening and riegel had similar, strongly correlated diurnal temperature cycles. Atmospheric-pressure measurements were taken from a barograph at Tarfala station in the valley below the glacier and corrected to glacier height using a temperature-compensated form of the altimeter equation. Corrections for atmospheric density had minimal effects on the timing and placement of the speed peaks and valleys discussed here; uncorrected measurements used for preliminary graphs in the field showed mostly the same results.

The distance meters used in these experiments have a stated absolute accuracy of 6–9 mm over the distances measured here. The ADM experiments depend upon the relative accuracy of a succession of measurements being more precise than this. That is, any systematic errors in a distance meter must affect successive measurements similarly and hence have a very small effect on their first time derivative. Each data point recorded by an ADM consisted of an average of three distance measurements, recorded to the nearest millimeter. Normally, the glacier does not move 1 mm during every 10 min interval, and random errors cause the measurements to fluctuate up and down 1–2 mm. The unsmoothed distance measurements thus produce a quantitized set of velocities, as the glacier appears to move −1, 0, 1 or 2 mm in each 10 min interval. Smoothing is necessary to turn these measurements into usable velocity data.

The smoothing method used here, as in Hanson and Hooke (1994), is an error-correcting cubic spline applied to distance data (routine DCSSMH in IMSL, 1994). More precisely, the spline is applied to distance data from which a trend line has been removed and hence it smoothes deviations from the average velocity of the entire record. Smoothing was tuned by specifying what percentage of the standard deviation of the detrended data consisted of error. Lacking an objective criterion for this smoothing parameter, we have used for each ADM series the minimum smoothing that removes negative velocities. In the resulting velocity curves, the timing and duration of major velocity fluctuations are insensitive to the smoothing parameter (Fig. 2). However, the absolute amplitudes of fluctuations

https://doi.org/10.3189/S0022143000002689 Published online by Cambridge University Press

shown here are uncertain, even though one can compare the relative amplitudes of different velocity fluctuations in the same series.

Series SR 92 and SR 93 are measurements of strain rates, for which negative values are possible. Strain rates are graphed and discussed here as rates of compression, in mm d^{-1}, between S2 and S3, so that the strain-rate curve can also be interpreted as a simple speed-difference curve. The strain-rate series were smoothed by forcing their qualitative appearance, in frequency and duration of graphically visible fluctuations, to mimic that of the corresponding velocity series for S3. Vector summing the S2–S3 strain rate with the S3 velocity in these cases yields slightly negative velocities for S2 during extreme compressional strain events, indicating that at least one of the series was undersmoothed.

Smoothing techniques are inherently subjective, but the method used here does little violence to the spectrum of variations, and it preserves the timing of peaks and valleys better than low-pass spectral smoothing methods. If integrated over time, this method reproduces the total observed motion of a stake. Our smoothing procedure is substantially more stringent than methods used in Columbia Glacier ADM experiments, reported by Walters and Dunlop (1987) and Meier and others (1994), as the order-of-magnitude smaller velocity on Storglaciären produces a noisier distance-meter dataset.

ADM raw data were obtained at unevenly spaced times, as the 10 min intervals mentioned above were times between attempted measurements, not necessarily between obtained measurements. Furthermore, with cubic-spline smoothing techniques, there is no particular advantage in calculating first derivatives directly at the raw-measurement times. Therefore, for calculational and graphical convenience, speed data were extracted at an evenly spaced time grid with 0.01 d intervals.

Water-pressure measurements

Each year, a number of holes was drilled through the glacier near S2 and S3 with the use of a hot-water drill. Most of these were for an investigation of the till layer beneath the ice but water-pressure transducers were installed in some (Table 1). Rustrak Ranger data loggers were used in 1991 and 1992. These, however, proved to be unreliable, particularly in 1992 and, in addition, they sampled data at a time grid of their own choosing, using a proprietary algorithm that is not available to us. Hence, the few data extracted from these devices were interpolated to the same 0.01 d time grid as the velocity data using cubic-spline interpolation (not smoothing).

In 1993, water pressures were measured again at S2 and S3 (using other data loggers) and also at an intermediate location dubbed S2.5. The longest available water-pressure series was from S2.5, as the series at S2 ended early when the borehole became disconnected from the conduit system and the series at S3 both started late and failed early. During a few days of overlapping records among these three locations, we were unable to detect a significant or consistent timing difference among them. That is, no evidence for propagation of a water-pressure wave was seen, although this conclusion is based on an unfortunately short period of overlapping record and on measurements over a relatively small distance (<300 m). In 1994, S2 and S0 were instrumented with pressure transducers and these were trouble-free. Even over this greater distance (>700 m), there is little evidence of a water-pressure wave propagating between the two sites. Although 1993 and 1994 data were mostly measured at 10 min intervals, these were also interpolated to a 0.01 d time grid for correlation with other data series.

ANALYSIS

Velocity- and water-pressure peaks

Lagged correlations

The common 0.01 d time grid allowed calculation of direct correlations as well as correlations at all possible lags within ±2 days for various pairs of time series (Table 3). Looking first at correlations between water-pressure series and their corresponding or nearby surface speeds (first block in Table 3), the best positive correlations are always obtained with a negative lag, meaning that increases in velocity normally preceded local increases in water pressure. These lags in the less-expected direction were as much as a quarter day in 1991 but were usually less than that.

Iken's (1981) modeling suggested that speeds may be highest on rising water pressures while subglacial cavities are expanding. Iken and others (1983) found field support for this idea on Unteraargletscher using approximately daily speed measurements but only for periods during which water pressures were extremely high. Using our finer time-scale data, lagged correlations with surface speed were calculated for the first-time derivative of the water-pressure series. This set of lagged correlations also showed peaks in surface speed generally preceding peaks in dp_w/dt and rises in surface speed often began while the local water pressure was still falling.

The correlations presented in Table 3 are for the entire season. Pearson correlations are always strongly influenced by a few large values, in this case the large, precipitation-induced velocity events. These events, in turn, have the least

Table 3. Summary of lagged and unlagged correlations among water pressure, velocity and strain-rate measurements. A range of ± 2 days of lag was explored in each case. Lags are given in days and correlations (R) in per cent

Forcing series	Lagged series	Zero lag	Absolute best		Best positive	
		R	Lag	R	Lag	R
WP 91–6	V 91–S2	+33	−0.26	+66	−0.26	+66
WP 92–1	V 92–S3	+77	−0.07	+79	−0.07	+79
WP 92–3	V 92–S3	+39	−1.55	−47	−0.11	+41
WP 93–1	V 93–S3	+72	−0.03	+72	−0.03	+72
WP 93–3	V 93–S3	+58	−0.17	+61	−0.17	+61
WP 93–5	V 93–S3	+23	−1.10	−41	−0.13	+28
WP 94–2	V 94–S2	+43	−0.11	+47	−0.11	+47
WP 92–1	SR 92	+35	+1.24	−38	−0.08	+35
WP 92–3	SR 92	+31	−2.00	−37	−0.17	+33
WP 93–1	SR 93	−60	+0.17	−63	−1.47	+50
WP 93–3	SR 93	-24	−0.35	−37	+1.24	+10
WP 93–5	SR 93	-11	−1.40	−40	+1.12	+15
V 92–S3	SR 92	-04	+0.70	+46	+0.70	+46
V 93–S3	SR 93	-29	−1.49	+37	−1.49	+37
V 94–S0	V 94–S2	+37	-0.17	+46	-0.17	+46

https://doi.org/10.3189/S0022143000002689 Published online by Cambridge University Press

reliability as to their exact timing, because the distance meters were unable to "see" their targets during heavy rainfall. The full-season correlations could thus be misleading. Correlations among shorter time series with smaller, diurnal signals revealed less consistency in either size or direction of the lagged correlations. However, examining stretches of these smaller, diurnal variations in Figure 2, one can see many cases where a velocity minimum precedes a water-pressure minimum and a velocity peak precedes a water-pressure peak. These support the full-season calculations and the conclusion that local water pressure is not driving the surface speed.

There is a lack of agreement between these data and the results found by Jansson (1995), who found a good correlation between effective pressure $(p_i - p_w)$ and surface speed (u_s): $u_s = 30(p_i - p_w)^{-0.4}$ (pressures in MPa, speeds in mm d^{-1}). Some of Jansson's measurements were made in the vicinity of S2, the rest were separated from ours by a series of large crevasses and the riegel. Jansson's velocity data were based on daily conventional surveys rather than ADMs and thus were of much lower time resolution. Furthermore, his high correlations were obtained for incidents in which high water pressures were maintained over a period of several days. We aggregated our data temporally to see whether results similar to Jansson's would result. Smoothing yielded slight improvements in some of the correlations shown in Table 3 but nothing like his 90% R^2 value was approached.

Composite diagrams

By inspection of Figure 2, we selected several days in each year during which all data series were available for the entire day without interpolating over data gaps. The days were not necessarily contiguous. (To produce a reasonable composite, some days with no water-pressure records were included in 1992.) Days chosen from each year were stacked to produce a number of composite single days (Fig. 3). Days with large precipitation were excluded; they are small in number and unique in character.

For 1991, Figure 3a shows the calculated quarter-day lag (Table 3) in that a velocity peak at 10.30 h was followed by a broad water-pressure peak at 16.00–19.00 h. The water-pressure peak is easily understood in terms of the diurnal melt cycle; the velocity peak in mid-morning is less easily understood. The 1994 measurements (Fig. 3e) show a similar water-pressure cycle (note the change in water-pressure scale between Figure 3a and e) but a much later S2 speed cycle. However, speed still leads water pressure in the 1994 diagram.

Graphical composites for 1992 and early season 1993 (Fig. 3b and c), when the speed measurements were at S3, are a little more ambiguous owing to lower coherence in both water pressure and velocity. Relatively small diurnal speed cycles are a feature of all S3 composites, implying that this area does not respond strongly or coherently to water inputs. Speeds tend to lead water pressures but not as dramatically as in the data from S2 (Fig. 3a and e). Water pressures in the 1992 composite (Fig. 3b) have a tiny amplitude but the deepest valley and highest peak are at times similar to other years.

To further summarize the 1991–93 graphs, a multi-year composite was created, in which all of the days included in Figure 3a–c were averaged (Fig. 4). In this stacking, S2 speeds for 1992 and 1993 were estimated by summing the

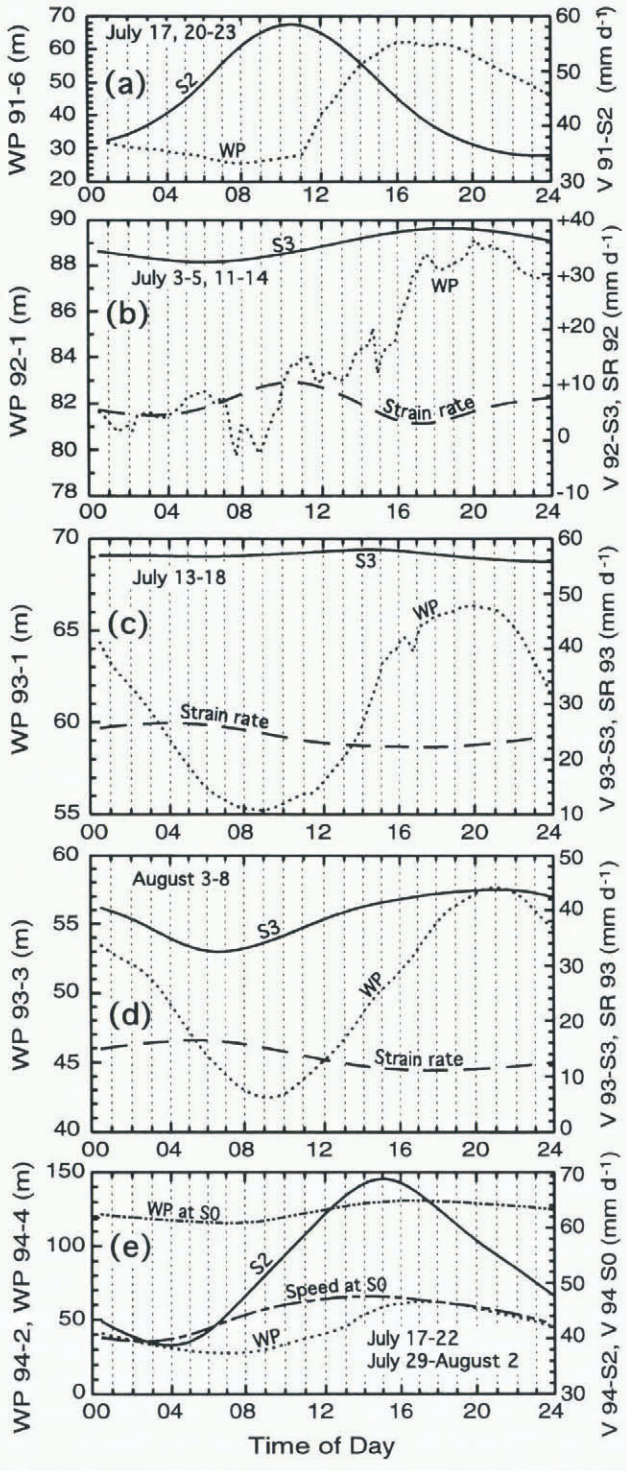

Fig. 3. One-diurnal-cycle composite diagrams, constructed by stacking the days listed on each figure. Curve types are the same as in Figure 2: solid is speed, dashed is strain rate, dotted is water pressure, with additional S0 curve types labelled in (e). Water pressures are given as height above the bed of the water level in the borehole: (a) 1991; (b) 1992; (c) 1993 early season; (d) 1993 late season; (e) 1994.

S3 speed and the strain rate for those years and averaging the results with the 1991 data. (This procedure, while conceptually accurate, is only a rough estimate of S2 speeds, because of the different and uncertain smoothing procedures used for strain-rate and velocity curves. If the method were perfect and the periods averaged in all three curves were the same, then the strain-rate curve shown in Figure 4 would be exactly the difference between the two velocity curves.)

https://doi.org/10.3189/S0022143000002689 Published online by Cambridge University Press

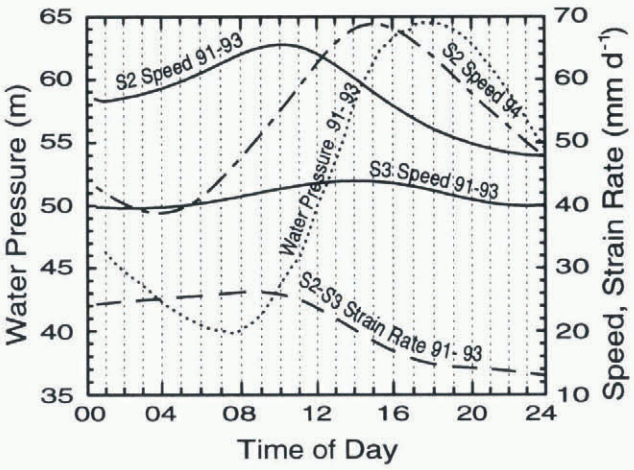

Fig. 4. One diurnal cycle in which curves labelled "91–93" were created by averaging together the days in Figure 3a–c for S2 and S3 early season, including S2 velocities estimated by adding S3 speed to S2–S3 strain rate for 1992 and 1993. The velocity curve for 1994 is the same as that in Figure 3e. Water pressures are given as height above the bed of the water level in the borehole.

The 1994 speed data from S2 were substantially more coherent diurnally than previously measured (1991) or calculated (1992–93) S2 speeds. If the 1994 data were averaged with those from the preceding 3 years, the resulting curve would look essentially like the 1994 curve, albeit damped. The 1994 curve was added to Figure 4 for comparison but left as a separate curve rather than included in the 1991–93 average. The 1994 S2 water-pressure composite (Fig. 3e) has identical timing and nearly identical amplitude (note again the scale change) to the 1991–93 water-pressure curve shown in Figure 4, so it was omitted.

Although Figure 4 is restricted to days that visibly showed diurnal cycles, it reinforces the correlation results. To the extent that we can find diurnal water-pressure cycles, they are remarkably consistent in all locations and in all years, with a late-afternoon peak and an early-morning minimum that are consistent with melt input driven by a diurnal temperature cycle. Timing and amplitude of velocity cycles are less consistent inter-annually and between locations but, in all cases the peak speed occurs earlier in the day than the peak water pressure, both at S2 and at S3, but most noticeably at S2.

Strain rates between S2 and S3

Simultaneous measurements of both S3 speed and S2–S3 strain rate from 1992 and 1993 clearly show that peak speeds at S2 precede those at S3. In the composite diagrams (Fig. 3b and c), this is shown by the consistency with which a peak in compressive strain rate precedes peak speed at S3, indicating a push from behind at S3. These composites include only a few days, restricted to early season in the 1993 case, but the same result can be inferred from the lagged correlations over the entire measurement period. The best positively correlated lags between S3 speed and S2–S3 strain showed lags of 0.7 and −1.5 days, respectively (Table 3). If we allow shifting the indicated lags by ±1 day to correlate proximal peaks with each other, then strain-rate peaks lead S3 speed peaks by 0.3–0.5 days.

Figure 4 includes S2 speeds inferred from the combination of S3 speed with S2–S3 strain rate. Both stake velocities begin to rise in the morning while water pressure is still rising. The more rapid acceleration at S2 creates a compression peak in the strain-rate curve at about 09.00 h that is then dissipated both by the ongoing acceleration of S3 and the decreasing acceleration of S2. By the time S3 reaches its velocity peak in mid-afternoon, both S2 speed and the strain rate have decreased sharply.

Although the timing of the onset of acceleration at S3 is consistent with rising strain rate, the onset of deceleration does not have a consistent timing with respect to the decreased strain rate. We can conclude that S3 begins its acceleration with a push from behind but it is not necessarily slowed by the decrease in magnitude of that push later in the day. Another implication of this inconsistency is that we cannot say whether the pushing of S3 consistently blocks the further acceleration of S2 or whether the ongoing motion of S3 sometimes decreases the back-pressure on S2.

As noted above, the 1994 S2 speed peak is much later in the day than in the previous 3 years. Even though it maintains its timing with respect to water pressure, the peak in S2 speed in 1994 nearly matches the timing of S3 speed peaks from 1992 and 1993. In the field, we noted that 1994 was an unusual year in that fewer crevasses opened up-glacier from S2 and new crevasses appeared elsewhere. We lack measurements that would confirm whether the pattern of ice S2 pushing ice at S3 was maintained in 1994.

DISCUSSION

Early season stress coupling

We generally see that velocities begin to increase before water pressure. The implication is that changes in the local velocity are driven by changing conditions elsewhere on the glacier, with speed conveyed to the region via stress coupling. Speculation on how this operates is significantly constrained by the presence of crevasses just up-glacier from the study area: a clear sign of extending flow.

Force-balance calculations for the area of the glacier in the vicinity of S2 (Hooke and others, 1989) suggest that during the winter about 20% of the driving force is balanced by side drag, 20% by a longitudinal stress gradient and 60% by basal drag. The longitudinal stress gradient arises from a combination of extending strain up-glacier from S2 and compressive strain down-glacier from it. The driving force is effectively constant on the time-scales we are considering. Hence, if we assume that changes in basal drag not responsible for initiating surface-velocity fluctuations (since water pressure is not changing appropriately), accelerations at S2 must result from: (1) decreases in side drag, (2) decreases in longitudinal pull from up-glacier, or (3) decreases in longitudinal back-pressure from down-glacier. The strain rate between S2 and S3 normally becomes more compressive as S2 accelerates (Fig. 4), so we can eliminate the third possibility.

Accelerations at S2 via reduction in side drag cannot be eliminated as a possibility but are unlikely. On the north side, water emerging from the glacier has a low sediment content, indicating little basal contact, and water emerges quite high along the left margin. On the south side, the lateral position of the largest surface-water inputs suggests that the large conduits are very near the margin where ice is thinner. It is thus unlikely that they are pressurized.

https://doi.org/10.3189/S0022143000002689 Published online by Cambridge University Press

The remaining potential source of acceleration at S2 is reduction in longitudinal tension due to accelerations up-glacier from S2. This is consistent with the 1994 measurements, showing that accelerations at S0 lead those at S2 (Fig. 3e). The small acceleration at S0 is insufficient to cause the larger one at S2 but S0 is off to the side of the glacier, so the magnitude of its acceleration may not be representative of what is happening along the center line. Hooke and others (1989) observed that compression can occur in areas of normally extending flow just down-glacier from the riegel during high water-pressure events that last a few days. That further supports the suggestion that reduction in tensile stress across the riegel is responsible for the acceleration of S2.

Pressures in the overdeepening up-glacier from S2 are consistently high (Hooke and Pohjola, 1994). Diurnal water-pressure variations found at S0 in 1994 typically had amplitudes of only 10–15 m (Fig. 2d). Although these are small, they are superimposed on water pressures that are often near overburden, so the small fluctuations must have a disproportionate effect on surface speed. We therefore conclude that early-season velocity changes at S2 are driven by speed changes in the main overdeepening above the riegel.

Late-season conduit development

In past years (Hooke and others, 1983b, 1989), we have found that velocities, averaged over several days, decreased gradually through the melt season and into the autumn. Such a pattern would be consistent with an evolution of the conduit system in which a better capacity for rapid through-put of water develops through the season, so that each succeeding water-input event will have less effect on the water pressure and hence velocity (Seaberg and others, 1988; Hock and Hooke, 1993; Iken and Truffer, 1997). The 1993 and 1994 measurement series were continued long enough into August to suggest that such a decrease might be starting but these measurements did not extend long enough to confirm it (Fig. 2c and d). Such behavior was also noted by Jansson (1995) for water pressures above the riegel in the summer of 1987. He found that he could not detect late-season water-pressure fluctuations in response to the diurnal temperature cycle. Only water inputs from precipitation events were large enough to show in the record.

Some observations relevant to the intra-seasonal development of the subglacial drainage system below the riegel were made in late July 1992 at S3. By 20 July, several holes had been drilled to the bed. Water levels in most of them had remained within 1 m of the glacier surface since completion. In the morning of 20 July, dirty water was observed emerging from two holes. The following day, a plug of frazil ice had formed in a third hole. When this was broken, slightly dirty water began to flow from the hole at a rate of about 1.6 l s^{-1}. On 22 July, a stormy day with wind and 33 mm of rain, dirty water was still emerging from another hole, although two of the others had stopped flowing. Then, on 23 July, all holes had drained. Observations on 24 July suggested that water levels were as much as 70 m below the surface in some.

From these observations, we infer that at this location and in the small overdeepening up-glacier from it (Fig. 1), the ice–bed interface was effectively impermeable before 20 July. This is consistent with our understanding of water flow through such overdeepenings (Hooke and Pohjola, 1994). Most of the subglacial water flow from the moulin area over the riegel probably flowed southward to join a branch of subglacial Sydjåkk that, as noted, we suspect runs at a relatively shallow depth along the south side of the glacier (Fig. 1). As the melt season progressed, high water pressures along this course probably gradually pried open small conduits leading through the shallow overdeepening and more directly to the terminus. This conduit system, we hypothesize, reached the vicinity of S3 during the night of 19–20 July, resulting in the excess pressures that produced artesian flow. The storm on 22 July then, we suppose, caused the conduit system, which had by this time reached areas somewhat down-glacier from the overdeepening to extend rapidly to the terminus, draining the holes.

Although drainage systems change continuously, major water-pressure events cause a proportionally greater increase in conduit capacity. In 1993, for example, there were a few major storm-induced high water-pressure events, two of which occurred between the series of days covered by Figure 3c and d, respectively. The timing and amplitude of the diurnal water-pressure cycle are basically the same before and after these events, but the amplitude of the diurnal speed cycle at S3 and of the S2–S3 strain-rate cycle increase markedly after the storms. Furthermore, the speed peak at S3 occurs later in the day and *is now in phase with the water-pressure peak*! Observations at S2 were similarly in phase with those at S3 in this late-season situation, as can be seen by the corresponding peak and valley of speed at S3 and strain rate at S2–S3 strain rate in Figure 3d.

We conclude from these observations that subglacial cavities were probably more interconnected after the mid-season storms in 1993 and that high water-pressure events thus affected a larger fraction of the glacier bed. This reinforces a conclusion recently reached by Iken and Truffer (1997), who found that the relation between speed and water pressure on Findelengletscher had changed dramatically between 1982 and 1994; they attributed the change to a change in the degree to which subglacial cavities were hydraulically interconnected and thus responding simultaneously to changes in water pressure.

In other words, on any given glacier, even holding the driving stress constant, it is unlikely that there is a unique relation between speed and water pressure. Equation (1) therefore needs to be modified to include a term describing the coherence of the hydraulic system. Jansson's (1995) data, demonstrating that at comparable water pressures sliding speeds on Storglaciären and Findelengletscher vary by an order of magnitude, are probably a manifestation of the same phenomenon.

CONCLUSIONS

Based on four summers (1991–94) of correlated water-pressure and speed measurements at two locations down-glacier from a large riegel on Storglaciären, we did not find a consistent relation between surface speed and water pressure. During small water inputs resulting from normal diurnal melt cycles, the up-glacier point (S2) accelerates first and pushes the down-glacier point (S3), but the initial acceleration of S2 cannot be explained in terms of local water pressure. The probable solution is that water pressure above the riegel rises earlier and that the resulting accelerations there allow S2 to accelerate via a relaxation of extensional stress.

https://doi.org/10.3189/S0022143000002689 Published online by Cambridge University Press

In the late season of 1993, after several large precipitation events that probably opened the drainage system, water-pressure peaks and surface-speed peaks coincided. Thus, as the water system becomes more integrated and coherent, the glacier begins acting more like idealized models of glacier sliding. Current sliding laws do not explicitly recognize the possibility of temporal changes in coherence of the subglacial hydraulic system.

ACKNOWLEDGEMENTS

P. Cutler and R. Hock provided meteorological data for distance-meter correction. We also thank our collaborators in the field during these experiments: N. Iverson, P. Jansson and J. Kohler. Thanks are due to P. Jansson for his computerized Storglaciären map that we adapted to Figure 1 and to U. Fischer for helpful comments on the manuscript. In addition, we relied on field assistance from J. Johansson, H. Laudon, B. Norell and J. Peterson. This research was financed by U.S. National Science Foundation grants DPP-86-19086, INT-87-12749, DPP-88-22156, OPP-92-24209, OPP-92-24175 and INT-92-13833, the Swedish Natural Sciences Research Council and the University of Delaware Research Foundation.

REFERENCES

Blake, E.W., U. H. Fischer and G. K. C. Clarke. 1994. Direct measurement of sliding at the glacier bed. *J. Glaciol.*, **40**(136), 595–599.

Brand, G., V. Pohjola and R.LeB. Hooke. 1987. Evidence for a till layer beneath Storglaciären, Sweden, based on electrical resistivity measurements. *J. Glaciol.*, **33**(115), 311–314.

Cutler, P. 1997. Water input and subglacial tunnel evolution at Storglaciären, northern Sweden. (Ph.D. thesis, University of Minnesota, Minneapolis)

Eriksson, M., H. Björnsson, U. C. Herzfeld and P. Holmlund. 1993. *The bottom topography of Storglaciären: a new map based on old and new ice depth measurements, analyzed with geostatistical methods.* Stockholm, Stockholm University. Department of Physical Geography. (Forskningsrapportserien STOU-NG 95.)

Hanson, B. 1995. A fully three-dimensional finite-element model applied to velocities on Storglaciären, Sweden. *J. Glaciol.*, **41**(137), 91–102.

Hanson, B. and R. LeB. Hooke. 1994. Short-term velocity variations and basal coupling near a bergschrund, Storglaciären, Sweden. *J. Glaciol.*, **40**(134), 67–74.

Hock, R. and R. LeB. Hooke. 1993. Evolution of the internal drainage system in the lower part of the ablation area of Storglaciären, Sweden. *Geol. Soc. Am. Bull.*, **105**(4), 537–546.

Hodge, S. M. 1974. Variations in the sliding of a temperate glacier. *J. Glaciol.*, **13**(69), 349–369.

Holmlund, P. 1987. Mass balance of Storglaciären during the 20th century. *Geogr. Ann.*, **69A**(3–4), 439–447.

Holmlund, P. 1988. Is the longitudinal profile of Storglaciären, northern Sweden, in balance with the present climate? *J. Glaciol.*, **34**(118), 269–273.

Holmlund, P. and M. Eriksson. 1989. The cold surface layer on Storglaciären. *Geogr. Ann.*, **71A**(3–4), 241–244.

Hooke, R. LeB. and V. A. Pohjola. 1994. Hydrology of a segment of a glacier situated in an overdeepening, Storglaciären, Sweden. *J. Glaciol.*, **40**(134), 140–148.

Hooke, R. LeB., J. E. Gould and J. Brzozowski. 1983a. Near-surface temperatures near and below the equilibrium line on polar and subpolar glaciers. *Z. Gletscherkd. Glazialgeol.*, **19**(1), 1–25.

Hooke, R. LeB., J. Brzozowski and C. Bronge. 1983b. Seasonal variations in surface velocity, Storglaciären, Sweden. *Geogr. Ann.*, **65A**(3–4), 263–277.

Hooke, R. LeB., S. B. Miller and J. Kohler. 1988. Character of the englacial and subglacial drainage system in the upper part of the ablation area of Storglaciären, Sweden. *J. Glaciol.*, **34**(117), 228–231.

Hooke, R. LeB., P. Calla, P. Holmlund, M. Nilsson and A. Stroeven. 1989. A 3 year record of seasonal variations in surface velocity, Storglaciären, Sweden. *J. Glaciol.*, **35**(120), 235–247.

Hooke, R. LeB., V. A. Pohjola, P. Jansson and J. Kohler. 1992. Intra-seasonal changes in deformation profiles revealed by borehole studies, Storglaciären, Sweden. *J. Glaciol.*, **38**(130), 348–358.

Hooke, R. LeB., B. Hanson, N. R. Iverson, P. Jansson and U. H. Fischer. 1997. Rheology of till beneath Storglaciären, Sweden. *J. Glaciol.*, **43**(143), 172–179.

Iken, A. 1981. The effect of the subglacial water pressure on the sliding velocity of a glacier in an idealized numerical model. *J. Glaciol.*, **27**(97), 407–421.

Iken, A. and R. A. Bindschadler. 1986. Combined measurements of subglacial water pressure and surface velocity at Findelengletscher, Switzerland: conclusions about drainage system and sliding mechanism. *J. Glaciol.*, **32**(110), 101–119.

Iken, A. and M. Truffer. 1997. The relationship between subglacial water pressure and velocity of Findelengletscher, Switzerland, during its advance and retreat. *J. Glaciol.*, **43**(144), 328–338.

Iken, A., H. Röthlisberger, A. Flotron and W. Haeberli. 1983. The uplift of Unteraargletscher at the beginning of the melt season — a consequence of water storage at the bed? *J. Glaciol.*, **29**(101), 28–47.

IMSL. 1994. *FORTRAN subroutines for mathematical applications. Vol. 1.* Houston, TX, Visual Numerics Inc. ISML.

Iverson, N. R., B. Hanson, R. LeB. Hooke and P. Jansson. 1995. Flow mechanism of glaciers on soft beds. *Science*, **267**(5194), 80–81.

Jansson, P. 1995. Water pressure and basal sliding on Storglaciären, northern Sweden. *J. Glaciol.*, **41**(138), 232–240.

Jansson, P. 1996. Dynamics and hydrology of a small polythermal valley glacier. *Geogr. Ann.*, **78A**(2–3), 171–180.

Jansson, P. and R. LeB. Hooke. 1989. Short-term variations in strain and surface tilt on Storglaciären, Kebnekaise, northern Sweden. *J. Glaciol.*, **35**(120), 201–208.

Kamb, B. and H. Engelhardt. 1987. Waves of accelerated motion in a glacier approaching surge: the mini-surges of Variegated Glacier, Alaska, U.S.A. *J. Glaciol.*, **33**(113), 27–46.

Kohler, J. 1995. Determining the extent of pressurized flow beneath Storglaciären, Sweden, using results of tracer experiments and measurements of input and output discharge. *J. Glaciol.*, **41**(138), 217–231.

Meier, M. *and 9 others.* 1994. Mechanical and hydrologic basis for the rapid motion of a large tidewater glacier. 1. Observations. *J. Geophys. Res.*, **99**(B8), 15,219–15,229.

Schytt, V. 1959. The glaciers of the Kebnekajse-Massif. *Geogr. Ann.*, **41**(4), 213–227.

Schytt, V. 1981. The net mass balance of Storglaciären, Kebnekaise, Sweden, related to the height of the equilibrium line and to the height of the 500 mb surface. *Geogr. Ann.*, **63A**(3–4), 219–223.

Seaberg, S. Z., J. Z. Seaberg, R. LeB. Hooke and D. W. Wiberg. 1988. Character of the englacial and subglacial drainage system in the lower part of the ablation area of Storglaciären, Sweden, as revealed by dye-trace studies. *J. Glaciol.*, **34**(117), 217–227.

Walters, R. A. and W. W. Dunlap. 1987. Analysis of time series of glacier speed: Columbia Glacier, Alaska. *J. Geophys. Res.*, **92**(B9), 8969–8975.

Weertman, J. 1957. On the sliding of glaciers. *J. Glaciol.*, **3**(21), 33–38.

MS received 15 September 1997 and accepted in revised form 20 January 1998